JOURNAL OF MATERIALS SCIENCE **34** (1999) 587–591

The origin of microtwinning at low strains during low-cycle fatigue of Inconel 718 at room temperature

A. BHATTACHARYYA, G. V. S. SASTRY, V. V. KUTUMBARAO
Department of Metallurgical Engineering, Banaras Hindu University, Varanasi 221 005, India
E-mail: gvss@banaras.ernet.in

The low-cycle fatigue (LCF) behaviour of a Ni–Fe base superalloy Inconel 718 was studied at room temperature. Deformation mechanisms operating at different strain amplitudes were established by detailed transmission electron microscopy at various fractions of fatigue life. It was observed that there was an increase in the number of microtwins present in the microstructure with increase in number of cycles, *N*, at low strains, where very little slip activity was identified. The undeformed specimens contain a number of annealing twins in the microstructure which increased in number with increase in cyclic deformation. Electron microscopy also revealed the existence of grain-boundary ledges in the undeformed specimens. A typical region of the grain-boundary area of the deformed samples showed a front of microtwins in their "nascent" state, advancing from one grain into the other. It was concluded that in the low-strain regime, cyclic deformation was accommodated by forming new microtwin interfaces emerging from grain-boundary ledges present in the undeformed specimens.

1. Introduction

Inconel 718, is a nickel-iron base superalloy sometimes used as a gas turbine disc material. This is one of the few superalloys in which γ'' is the principal strengthening phase. Little information is available on the low-cycle fatigue (LCF) behaviour of this alloy, although LCF is an important service condition for disc materials. Earlier LCF investigations on IN 718 at room temperature have been reported by Merrick [1], Fournier and Pineau [2], Worthem *et al.* [3] and recently Rao *et al.* [4]. Merrick [1] investigated the LCF behaviour of the heat-treated alloy over a narrow range of strain amplitudes. A significant improvement in fatigue resistance was obtained by a reduction in grain size. A small degree of fatigue hardening was quickly followed by fatigue softening at room temperature. The fatigue softening was attributed to shear and subsequent dissolution of the precipitate (γ''). Fournier and Pineau [2] highlighted the LCF behaviour at room temperature at a single strain amplitude of about $\pm 1.0\%$. Electron microscopy revealed that the γ'' had been sheared during cyclic straining and that plastic deformation continued by the propagation of planar bands, which were identified as twins. However, Worthem *et al.* [3], who also studied the LCF behaviour of the commercially heat-treated alloy at a strain amplitude of $\pm 1.0\%$, found regularly spaced arrays of deformation bands on [1 1 1] slip planes but no twins. Recently, Rao *et al.* [4] examined the LCF behaviour of the alloy at the same strain amplitude of $\pm 1.0\%$, and observed that the cyclic deformation occurred primarily by planar slip. The microstructure showed the presence of slip bands and a few microtwins. In a systematic study of the LCF behaviour of the alloy at room temperature over a range of strain amplitudes marked by detailed and quantitative TEM examination of specimens at various stages of their fatigue lives, the present authors [5] established microtwinning to be the dominant mode of deformation at low strain amplitudes. This changes to planar slip in the high strain amplitude regime leading to dual slope Coffin–Manson (C–M) plot. The present paper reports the results of a detailed TEM study carried out to understand the origin of microtwins at low strains.

2. Experimental procedure

The material of the present investigation, Inconel 718, was obtained in the form of 15 mm diameter cold drawn bars which had been solution treated at 980 °C for 1 h followed by air cooling. The chemical composition of the as-received material is given in Table I.

The as-received rods were cut into 120 mm length blanks and were given a conventional double ageing treatment : ageing at 720 °C/8 h/furnance cooling to 615 °C/8 h/air cooling.

LCF tests were carried out on a computer-controlled servohydraulic MTS testing machine (Model-810) of ± 50 kN capacity. Fully reversed ($R = -1$) LCF tests were performed in air under total axial strain control. Six total strain amplitudes in the range $\pm 0.45\%$ to $\pm 1.25\%$ were used for tests carried out at a constant

TABLE I Composition (wt %) of the material of study

Cr	Ni	Mo	C	Ti	Al	Nb	Fe
18.71	53.63	3.0	0.027	1.02	0.5	5.26	Bal.

frequency of 0.1 Hz at room temperature. These tests were continued until fracture. Interrupted LCF tests were carried out for a predetermined number of cycles corresponding to half life ($N_f/2$), quarter life ($N_f/4$) and the observed maximum in the stress amplitude, respectively. The interrupted tests were conducted at three different total strain amplitudes namely, $\pm 0.625\%$, $\pm 0.8\%$ and $\pm 1.125\%$, at room temperature.

Thin foils for TEM examination were prepared from coupons cut from the gauge section perpendicular to the axis of the LCF test specimens. Thin foils for undeformed (e.g. as heat-treated) specimens were prepared from coupons cut from the 120 mm heat-treated blanks. The coupons were ground to a thickness of 0.025 mm. Discs, 3 mm diameter, were punched out from the ground coupons and jet polished to perforation in a 10% solution of perchloric acid in glacial acetic acid. Jet polishing was done at ambient temperature using a potential of 25 V. TEM observation of the thin foils was carried out using a Jeol JEM 200 CX microscope operated at 160 kV.

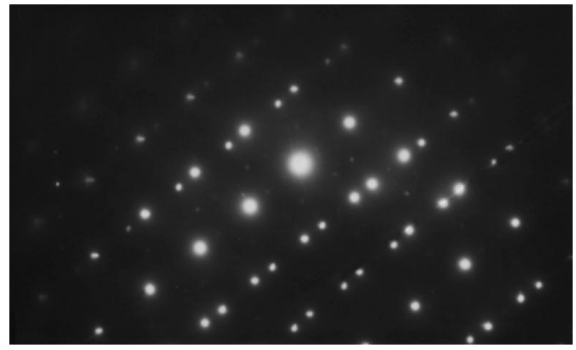

(a)

(b)

Figure 1 (a) Diffraction pattern showing (1 1 0) twins of f c c in $\pm 0.625\%$ strain amplitude specimen. (b) Bright-field micrograph of the same, $N_f/4$. Note the steps on the twin interfaces.

3. Results and discussion

At the lower strain amplitude of $\pm 0.625\%$ TEM study was conducted on specimens tested up to 5 cycles ($\Delta\sigma/2_{max}$), 1500 cycles ($N_f/4$) and 3000 cycles ($N_f/2$), respectively. The most significant microstructural features observed in these specimens were microtwins in increasing number (Fig. 1). The number of microtwin interfaces per grain increased with increasing number of cycles, N. Confirmation that the observed features were indeed twins was obtained as follows. The foils were tilted to [0 1 1] twin orientation and from the corresponding selected-area diffraction pattern (SADP) (Fig. la) twin spots were identified. Subsequently, dark-field (DF) images from one of the twin spots were taken which highlighted the twins as mentioned. Each step on the micro-twin boundaries was counted as one micro-twin interface. The microtwin interface density thus computed not only was significantly higher than that observed in the undeformed specimens, but also increased with number of cycles.

Apart from the above, no other significant features were seen. In particular, the dislocation substructure could not be imaged. No precipitate–dislocation interaction was observed even at the highest magnifications available on the microscope. The high coherency strain of 2.86% associated with the γ'' precipitate [6] may have obstructed the observation of detailed dislocation structure, as mentioned by Fournier and Pineau [2]. Thus, any direct signature of the small cyclic plastic deformation that the sample underwent was lost in the strain contrast associated with the precipitates.

Table II summarises the TEM observations on the LCF behaviour of Inconel 718 at room temperature. It may be emphasized here that such detailed

TABLE II Summary of TEM observations on interrupted LCF specimens at room temperature and at 0.1 Hz (average grain diameter $\sim 7\ \mu$m)

Strain amplitude (%)	No. of cycles at which test was stopped	Corresponds to	No. of twin interfaces/ grain, N_t	Approx no. of slip bands/ grain, N_s	Av. slip band spacing (μm)
0.625	5	$(\Delta\sigma_{max}/2)$	0.4	No slip band	—
	1500	$(N_f/4)$	0.6	No slip band	—
	3000	$(N_f/2)$	3.0	No slip band	—
0.800	2	$(\Delta\sigma_{max}/2)$	1.0	No slip band	—
	600	$(N_f/4)$	1.25	6.61	1.06
	1200	$(N_f/2)$	1.25	8.23	0.85
1.125	2	$(\Delta\sigma_{max}/2)$	0.7	Negligible	—
	200	$(N_f/2)$	1.1	10.61	0.66
Undeformed			0.3		

quantitative results on the density of twin interfaces and slip band spacing are reported perhaps for the first time in the open literature on LCF studies. It is evident from Table II that at the start of cycling at both low and high strain amplitudes, deformation is confined to the formation of additional interfaces along microtwin boundaries. However, on cycling until about half the life of the specimen, a change occurs. Now, cyclic deformation continues to be accounted for in the low-strain region mainly by an increase in the density of micro-twin interfaces, but in the high-strain regime, the deformation is accommodated principally by slip band formation. It may be observed that at half-life in the high-strain region, the microtwin interface density is about 1.1. This value may appear to be comparatively large, but it should be noted that it is only a third of that found in the specimens cycled to half-life at the lower strain amplitude of $\pm 0.625\%$. Thus it can be said that, in the high-strain region, the dominant mode of deformation is planar slip. The following questions arise as a result of these observations.

(a) How does the number of micro-twin interfaces increase with number of cycles in the low-strain region as compared to that obtained in the undeformed specimens?

(b) How is such an increase in micro-twin interface density helpful in accommodating the cyclic deformation in the low strain region?

An attempt has been made to find the answers to these questions.

3.1. Steps on microtwin interfaces

It should be mentioned that the undeformed specimens contain a number of annealing twins. Frequently steps have been observed on the coherent or parallel faces of the micro-twins in the deformed specimens. Sometimes such steps have also been seen on the non-parallel faces of the microtwins. This may be taken as an indication that cyclic deformation has been accommodated, at least partially, by the formation of the steps, as no such steps have been found in the undeformed specimens (Fig. 2). Confirmation of this idea has been obtained in the following way.

Fig. 3 shows stepped twins in the low strain regime at five cycles ($\Delta\sigma/2_{\max}$). Tracing of [1 1 1] from the corresponding diffraction pattern (Fig. 3a) on the stepped twin shows that [1 1 1] is perpendicular to the steps. It indicates that cyclic deformation is initially accommodated by the movement of existing twin interfaces in the {1 1 1} planes. The steps are observed to be going into the interface in some positions and going out of it in some other. Such differences may be attributed to the formation of these steps during tension and compression parts of the cycling, respectively.

It is also possible that twin precursors were present in the undeformed specimens and that during subsequent cycling these precursors propagated, leading to the observed features. Together with step formation on microtwins, this can explain the considerable increase in microtwin interface density observed in the LCF samples.

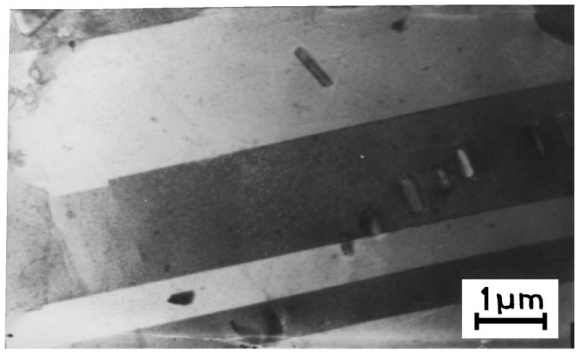

Figure 2 Bright-field image of the undeformed specimen showing twins without stepped interfaces.

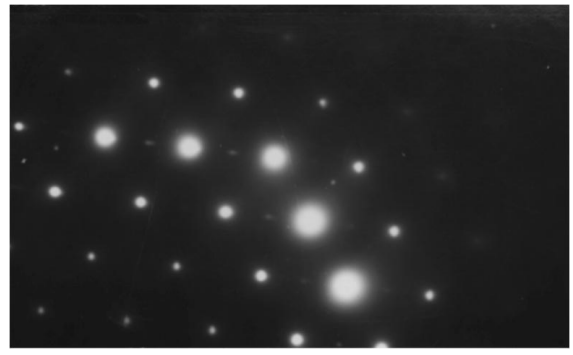

(a)

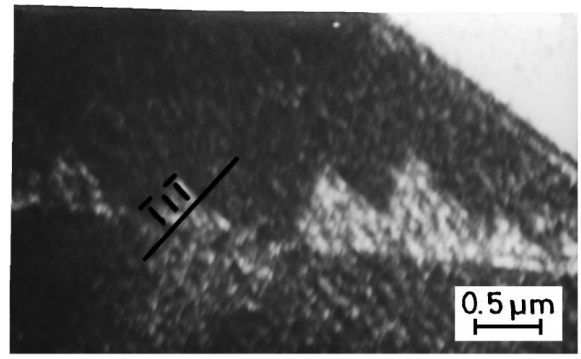

(b)

Figure 3 (a) Diffraction pattern and (b) Micrograph showing stepped microtwin boundaries in specimens of $\pm 0.625\%$ strain amplitude at $N = 5(\Delta\sigma_{\max}/2)$. The $[\bar{1}\,1\,1]$ vector is traced on the micrograph.

3.2. Origin of microtwin interfaces

To resolve the issue of whether twin precursors existed before deformation, further detailed TEM study has been undertaken. Grain-boundary ledges of reasonable dimensions (30 nm step height) (Fig. 4) could be seen in the undeformed specimens. A front of such microtwins in their "nascent" state, advancing from one grain to the next, is shown in Fig. 5a. A slightly different tilt position of the TEM foil has shown that the steps seem to be emanating from grain I (Fig. 5b). Orientation relationships of the grains I and II and the advancing steps have been carefully studied and established. The bright-field (BF) micrograph shown in Fig. 5a was obtained at zero tilt position of the sample in the holder. The foil normal

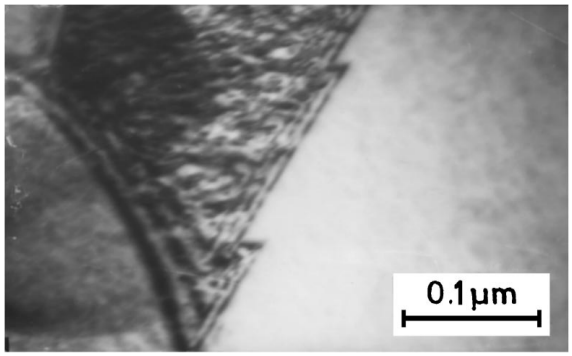

Figure 4 Bright-field image of the undeformed specimen showing grain-boundary ledges (step height $\simeq 30$ nm).

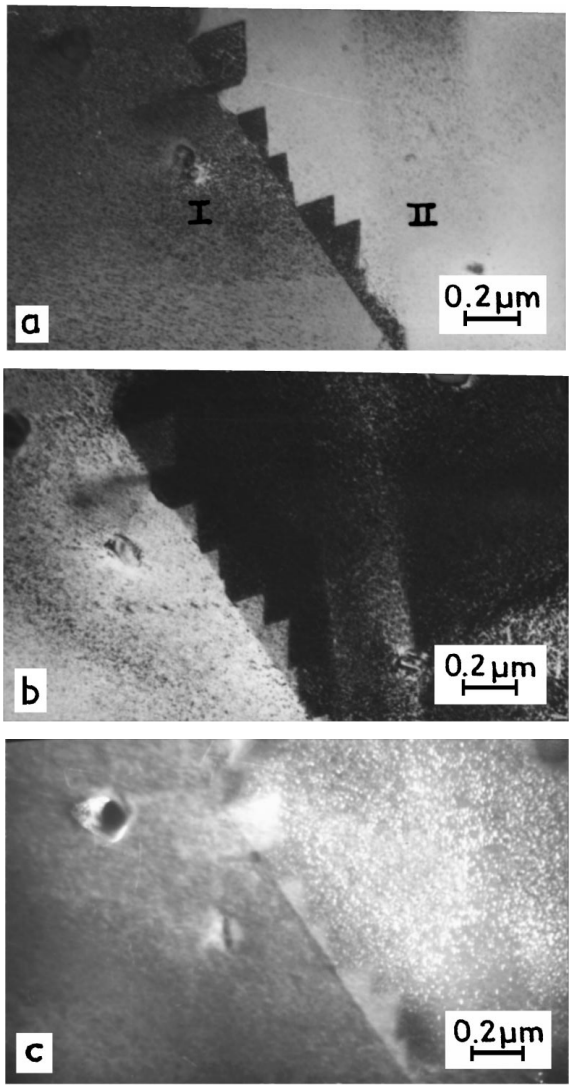

Figure 5 Transmission electron micrographs of samples at $\pm 0.625\%$ strain amplitude and $N_f/4$ showing (a) a stepped front emanating from a grain boundary (grain I) and advancing into an adjacent grain (grain II), (b) the same area at zero tilt position, and (c) at a tilt of 2° from the above position. Note that the stepped front goes out of contrast.

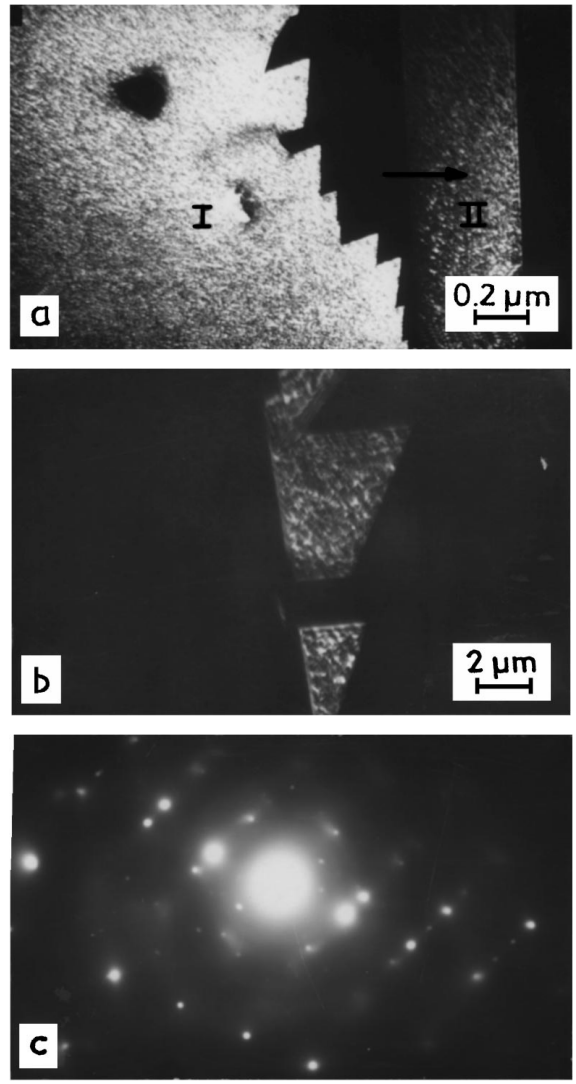

Figure 6 When further tilted to [1 1 0] orientation the DF micrographs show (a) grain I together with the stepped front and a twin in the grain II in contrast, (b) a stepped front having a twin relation with grain II, and (c) the corresponding SAD pattern.

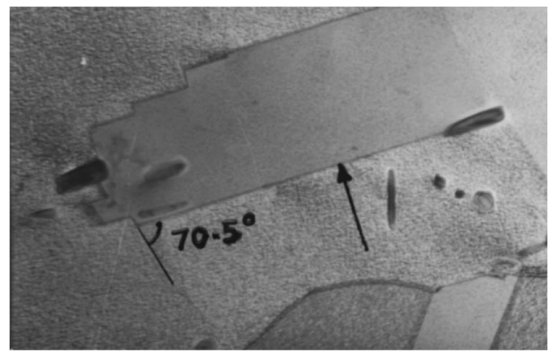

Figure 7 The (1 1 1) twinning planes of the stepped front make an angle 70.5° with (1 1 1) habit planes of the twin (marked by an arrow).

has been worked out to be [1 1 2] from the selected-area diffraction pattern (SADP) in that tilt position. A two-degree tilt from the zero position (Fig. 5c) caused the stepped front to go out of contrast, implying that the steps were at a very small tilt angle with respect to grain I. From this orientation the specimen was further tilted until grain I came into the [1 1 0] zone axis orientation. In this orientation, the dark-field (DF) micrograph (Fig. 6a) showed grain I together with the stepped front and a microtwin interface in grain II (marked by arrow) in contrast. This indicates that the advancing steps bear a twin relation to grain II. These interface relations also imply that grains I and II are twin-related. Many such twin-related grains have been observed in the cyclically deformed samples.

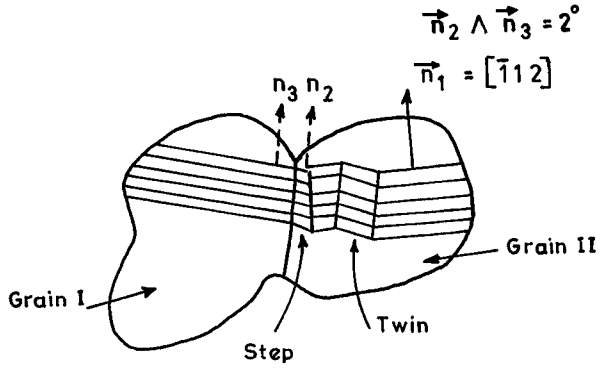

Figure 8 Schematic diagram showing orientation relation of the grains I and II and the steps emanating from grain I. Foil normal is [1 1 2]. The misorientation between grain I and the steps which have grown from the pre-existing ledges, is 2°.

The (1 1 1) twinning planes of the stepped front make an angle of 70.5° with the (1 1 1) twin habit planes of the twin marked by an arrow in (Fig. 7). This value is close to the expected angle of 70°32′ between two {1 1 1} planes in f c c. Further, the plane of the advancing front of these steps is straight and thus can be expected to be coherent. The dark-field micrograph and the diffraction pattern shown in Fig. 6b and c further corroborate the twin relation of the steps. A schematic drawing illustrating the various crystallographic relationships between the two grains and steps is given in Fig. 8, to present a clear picture of the proposed mechanism. Here the foil normal and relative orientations of the various positions are indicated schematically. It is proposed that the grain-boundary ledges already present in the undeformed specimens act as twin precursors and grow into micro-twins during subsequent cyclic deformation. Therefore, the cyclic deformation in the low strain region is not only accommodated by forming steps in the existing twins but also by forming new micro-twins emerging from grain-boundary ledges.

4. Conclusion

The deformation behaviour during LCF of the alloy Inconel 718 at room temperature (RT) in the low-strain regime can be summarized as follows.

In the low-strain region, cyclic deformation is accommodated by forming either steps in the existing microtwin interfaces or by forming new microtwin interfaces emerging from grain-boundary ledges present in the undeformed specimens. Together, these two mechanisms result in an increase in the number of microtwin interfaces per grain with increasing cyclic deformation.

Acknowledgement

This work has been carried out with financial assistance provided by the Council of Scientific and Industrial Research (CSIR), Government of India (Project No. 10(142)/90.EMR-II).

References

1. H.F. MERRICK, *Metall. Trans.* **5** (1990) 891.
2. D. FOURNIER and A. PINEAU, *ibid.* **8A** (1977) 1095.
3. D. W. WORTHEM, J. M. ROBERTSON, F. A. LECKIE, D. F. SOCIE and C. J. ALTSTETTER, *ibid.* **21A** (1990) 3215.
4. K. B. S. RAO, K. SREERAMESH, G. R. HALFORD and M. A. MCGRAW, *Scripta Metall.* **32** (1995) 493.
5. A. BHATTACHARYYA, G. V. S. SASTRY and V. V. KUTUMBARAO, *ibid.* **36** (1997) 411.
6. M. C. CHATURVEDI and FANG HAN YA, *Metal Sci.* **17** (1983) 145.

Received 21 January
and accepted 27 July 1998